# Photocatalytic cyanation of carbon nitride scaffolds: Tuning band structure and enhancing the performance in green light driven C—S bond formation

Lina Li, Daniel Cruz, Aleksandr Savateev, Guigang Zhang, Markus Antonietti, Yubao Zhao*

Department of Colloid Chemistry, Max-Planck Institute of Colloids and Interfaces, Potsdam 14476, Germany

## ARTICLE INFO

## ABSTRACT

A new photocatalytic reaction process is described that cyano groups (—CN) are successfully grafted on carbon nitride (g-$C_3N_4$ materials). The cyano group substitutes the previous surface terminating amino group (—$NH_2$) on g-$C_3N_4$ by a radical reaction pathway, modifying the electron structure of the conjugated covalent system and engendering favorable properties for the visible-light driven photocatalysis. Cyanidated g-$C_3N_4$ (g-$C_3N_4$-xCN) has a narrowed band gap of 2.29 eV, as compared to 2.73 eV for the pristine g-$C_3N_4$, showing expanded visible light absorbance to 590 nm. Moreover, the photo-induced charge-carrier separation is improved as well. In consequence, g-$C_3N_4$-xCN exhibits significantly enhanced performance in photocatalysis, here exemplified with the model coupling reaction towards alkenyl sulfones under green light (520 nm) irradiation. The methodology reported herein reveals the potential of the carbon nitride scaffold to be modified as such and illustrates the possiblities of the as-created novel carbon nitride materials grafted with various functional groups on their surface.

## 1. Introduction

Graphitic carbon nitride (g-$C_3N_4$), a fascinating conjugated polymer with visible-light sensitivity, good thermal and chemical stability, and non-toxicity, has attracted intensive research interest as a visible-light responsive photocatalyst for hydrogen evolution, water oxidation, carbon dioxide reduction, water pollutant degradation, and organic chemicals conversion reactions [1–7]. Despite of the versatility, carbon nitride photocatalytic systems still suffer from low efficiency for solar energy conversion. Much research efforts have been made to expand the visible light absorbance to longer wavelength, and to improve photo-induced charge separation, so as to further push the solar-light conversion efficiency upward [1,8,9]. Heteroatoms doping [10,11], controlled nanostructures/hierarchy structures fabrication [9,12], and hetero-junction design [13,14] are, so far, the most common strategies for ameliorating the current, sometimes unsatisfactory low efficiency [15–18].

The introduction of defects to carbon nitride is usually considered as an effective method to promote photocatalytic performance [19–21]. Recently, nitrogen deficient carbon nitride materials by introducing nitrogen defects in the framework was found to significantly expand the visible light response of such materials [22–24]. However, due to the well-known chemical stability of the carbon nitride, harsh reaction conditions are usually required for post-modification of the samples. An

alternative pathway with milder reaction condition and easier operations is to our opinion still desirable.

Given the conjugated system of the g-$C_3N_4$ and learning from the long history of dye chemistry, we believe that color can be tuned by expanding the conjugated systems with small donor and acceptor substituents [25,26]. We thus propose a strategy of grafting e.g. cyano groups on the g-$C_3N_4$ scaffold, thus lowering the relative nitrogen content chemically, as opposed to the previous approaches of reducing the nitrogen contents by partially destroying the g-$C_3N_4$ frameworks (and potentially creating the nitriles indirectly as leftover groups). The challenge here is, in spite of the known chemical/thermal stability of the tri-s-triazine unit and the carbon nitride, to develop efficient approaches for grafting the selected functional groups.

It has been reported that cyano groups can be photocatalytically grafted onto N-containing heterocyclic rings [27]. Moreover, thiocyanate salts, which could be converted to cyanides by oxidation, are widely used as a safe cyanation reaction reagent [28–30]. Inspired by those facts, we employed thiocyanate salt as the cyano group source via a facile photocatalytic reaction. In this strategy, the thiocyanate ion is first photocatalytically converted to cyano radical by carbon nitride; which recombines with the carbon nitride scaffold afterwards, forming cyanidated g-$C_3N_4$ (g-$C_3N_4$-xCN, where x represents the content of CN group in the sample by weight percentage). It is worth noting that the C/N ratio (or the CN group content in the sample) or the substitution

degree can be facilely controlled by varying the reaction conditions, such as irradiation time and NaSCN concentration of the reaction mixture. Most importantly, the band gap is directly affected by the cyano group content in g-C$_3$N$_4$-xCN. The samples with higher CN content show a narrower band gap. The band gap could be tuned down to 2.29 eV, as compared to 2.73 eV for the pristine g-C$_3$N$_4$, expanding the visible light response to an adsorption edge of 590 nm. It is shown that the photo-induced charge-carriers separation is improved as well, and that g-C$_3$N$_4$-xCN exhibits significantly enhanced performance under green light (520 nm) irradiation, as exemplified with a model reaction, the photocatalytic C−S coupling reaction towards alkenyl sulfones. This can be set in stark contrast with the negligible activity of the pristine carbon nitride at this wavelength.

## 2. Experiments

### 2.1. Preparation of parental carbon nitride

492 mg melamine and 514 mg cyanuric acid were mixed in 40 ml H$_2$O and stirred overnight. The mixture was then separated and dried in vacuum, followed by polymerization at 550 °C for 4 h in an oven with N$_2$ flow. The as synthesized yellow powder is simplistically called g-C$_3$N$_4$.

### 2.2. Cyanation of carbon nitride

The cyanidated carbon nitride samples with varying CN modification are denoted as g-C$_3$N$_4$-xCN, where x represents the content of CN group in the sample by weight percent. In a typical synthesis of g-C$_3$N$_4$-16CN, 60 mg g-C$_3$N$_4$ and 180 mg NaSCN are added to 20 mL acetonitrile in a 50ml photoreactor. The photoreactor was irridiated by 100W white LED for 8 h in air under room temperature. The solid product was collected and washed with H$_2$O and ethanol. For the samples with various CN contents, only the concentration of NaSCN was changed, while all other parameters are kept the same.

## 3. Results and discussion

As determined by elemental analysis, TEM-EELS characterization, and XPS analysis, there is no sulphur residue in the cyanated samples (Figs. S1–S3). The content of cyano groups in the sample increases with the concentration of NaSCN in the reaction mixture (Table S1), and the cyano group weight percentage can reach maximum value of 16% (C/N molar ratio of 0.664) (Fig. S4). Further increase of NaSCN concentration with elongated irradiation time cannot raise the C/N ratio any further, indicating that all the possible reaction sites on the carbon nitride scaffold have been substituted by cyano groups. This reaction can thereby be easily used to evaluate the incompleteness of the condensation of the tri-s-triazine units, and the as made polymeric carbon nitride is obviously rather a melon than a completely condensed g-C$_3$N$_4$.

To understand the changes in the framework structure of the carbon nitride scaffold caused by cyanation, the samples were characterized by Fourier-transform infrared (FTIR) spectroscopy. As shown in Fig. 1a, NaSCN shows a sharp absorption peak at 2100 cm$^{-1}$, while for all the g-C$_3$N$_4$-xCN samples, this peak is absent, which states that all the g-C$_3$N$_4$-xCN samples are free of NaSCN residues. It is worth noting that there are two distinctive peaks varying in intensity with the cyano group contents in the samples. One is the absorption peak at 2240 cm$^{-1}$, which is corresponding to the carbon-nitrogen triple bond (C≡N) vibration and is increasing with cyano group content in the sample. The other is the multiple broad peaks at 3000– 3300 cm$^{-1}$, which are usually assigned to the N−H stretching vibration of the amino group (−NH$_2$). With the increase of cyano group contents in the samples, this N−H vibration peak is massively diminished. These data strongly support the proposed substitution of amino group (−NH$_2$) by the cyano group (−CN). All the other typical vibration peaks of the g-C$_3$N$_4$ scaffold keep unchanged, indicating that the carbon nitride framework stays intact.

Moreover, the samples are also characterized by Raman spectroscopy. Due to very strong fluorescence background emission of the carbon nitride materials, the Raman vibration signal is extremely weak. However, we have captured the Raman vibration peak at 2240 cm$^{-1}$, which can be assigned to the CN group (Fig. S5). This signal increased with the content of the cyano group in the sample, which is consistent to the FTIR results.

The samples were also characterized by XRD to study the effect of the cyanation on the local structure of the samples (Fig. 1b). The diffraction intensity from the sample with higher cyano group content is lowered, but in spite of the changes in peak intensity, all the samples show the characteristic diffraction from (002) crystal plane at 27.5°, without any displacement. This states that the in-plane packing and inter-facial stacking situation of C$_3$N$_4$-xCN did not change at all; even the distance between layers is kept the same. There are no obvious changes on morphology of the samples before and after photocatalytic cyanation as shown by the SEM images (Fig. S6).

Changes of the surface composition of carbon nitrides with introduction of further cyano groups were followed by X-ray photoelectron spectroscopy (XPS) (Fig. 2). For pristine g-C$_3$N$_4$, there is one main C1s peak with binding energy of 288.5 eV, which represents the carbon in triazine ring (N−C≡N). After cyanation, two additional C1 s peaks appear at 286.9 eV and 285.2 eV. They are, respectively, corresponding to the carbon atoms in cyano group and the one in heptazine unit bonding with cyano group [31–32]. The intensity of the additional peaks increase with the content of cyano group in the sample, strongly demonstrating that cyano group has been successfully grafted on carbon nitride scaffold. For the N1 s curve (Fig. 2), the broad peak contain 3 components with binding energy peak at 402 eV (hydrogenated nitrogen), 400 eV (charge depleted amine), and 398 eV (nitrogen in double bond and triple bond with carbon) [33]. With the increase of the cyano group content in the samples, the intensity of the peak at 398 eV is increasing, while the peak at 402 eV is decreasing. This again confirms that the amino group on the g-C$_3$N$_4$ scaffold is successfully substituted by cyano group during photocatalytic cyanation process.

A series of control reactions were conducted for revealing the reaction mechanism of photocatalytic cyanation process. As shown in Table S1, light irradiation, NaSCN, and aerobic condition, are all prerequisites for the successful grafting of cyano group on the carbon nitride scaffold. This reaction was impeded in the presence of TEMPO (2,2,6,6-tetramethyl-1-piperidinyloxy) radical scavenger, which indicates that the cyanation reaction proceeded through a radical pathway. After the reaction, sulfate ions (SO$_4$$^{2-}$), which is one of the products of the thiocyanate ion (SCN$^-$) oxidation, are detected on the unwashed sample. Together with the above spectroscopic analysis, we thus propose a brief reaction mechanism. The aerobic photocatalytic oxidation of SCN$^-$ produces CN$^-$, which could be converted to cyano radical by photo-induced hole. The cyano radical can attack/recombine with the charged triazine ring and replace the amino group, releasing ammonium ions and affording cyanidated carbon nitride.

The effect of the cyanation process on the visible light response of the materials was studied by UV–vis absorbance spectroscopy. As shown in Fig. 3, the pristine g-C$_3$N$_4$ has an absorption edge at around 450 nm, and a significant red shift of the absorption edges is observed for the samples with increasing cyano group contents. The absorption edge of the sample g-C$_3$N$_4$-16CN extends to 590 nm, which is significant for a potential better absorption of the solar light spectrum. The band gap is calculated based on Tauc's plot. As shown in Fig. 3b, the band gap gradually decreases from 2.73 eV for the pristine g-C$_3$N$_4$ to 2.29 eV for g-C$_3$N$_4$-16CN. The colour of the samples thus changes gradually from pale yellow to gold, as shown in the insets in Fig. 3b.

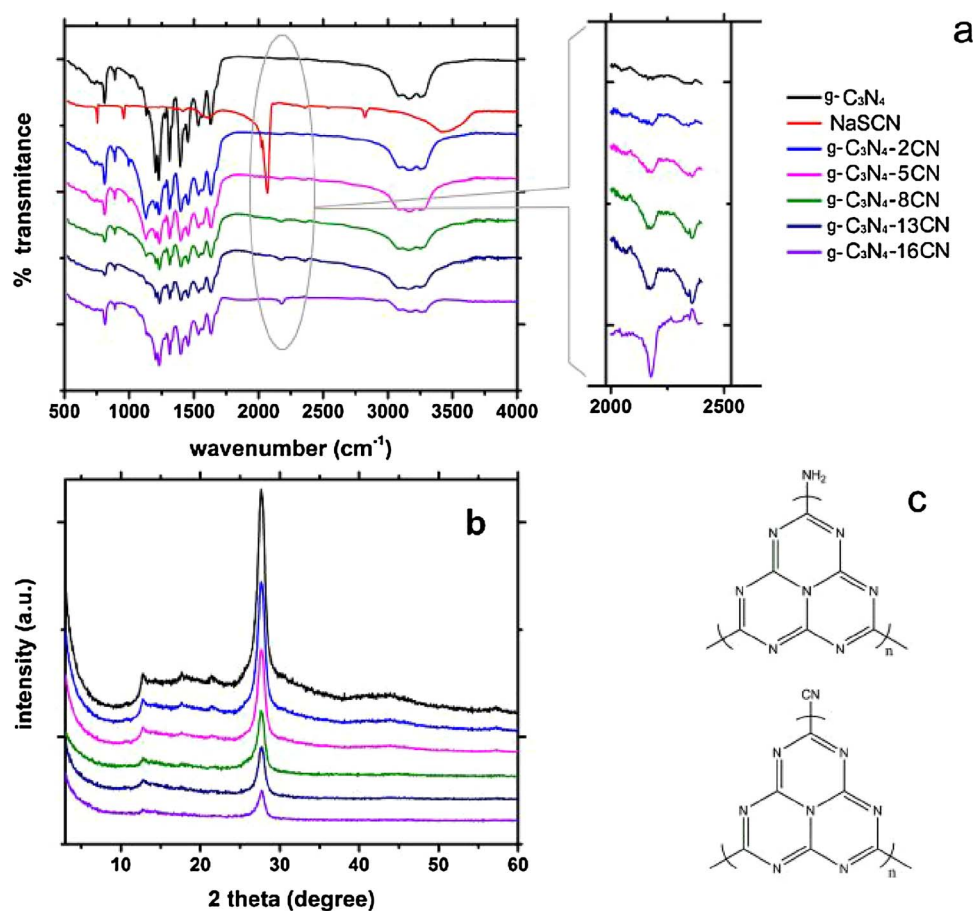To determine the valence band level, the cyanated g-C$_3$N$_4$ samples

Fig. 1. Fourier-transform infrared (FTIR) spectra (a), X-ray diffraction (XRD) patterns (b) of g-C$_3$N$_4$-xCN samples. (c) Proposed structural change in heptazine units before and after the photocatalytic cyanation reaction.
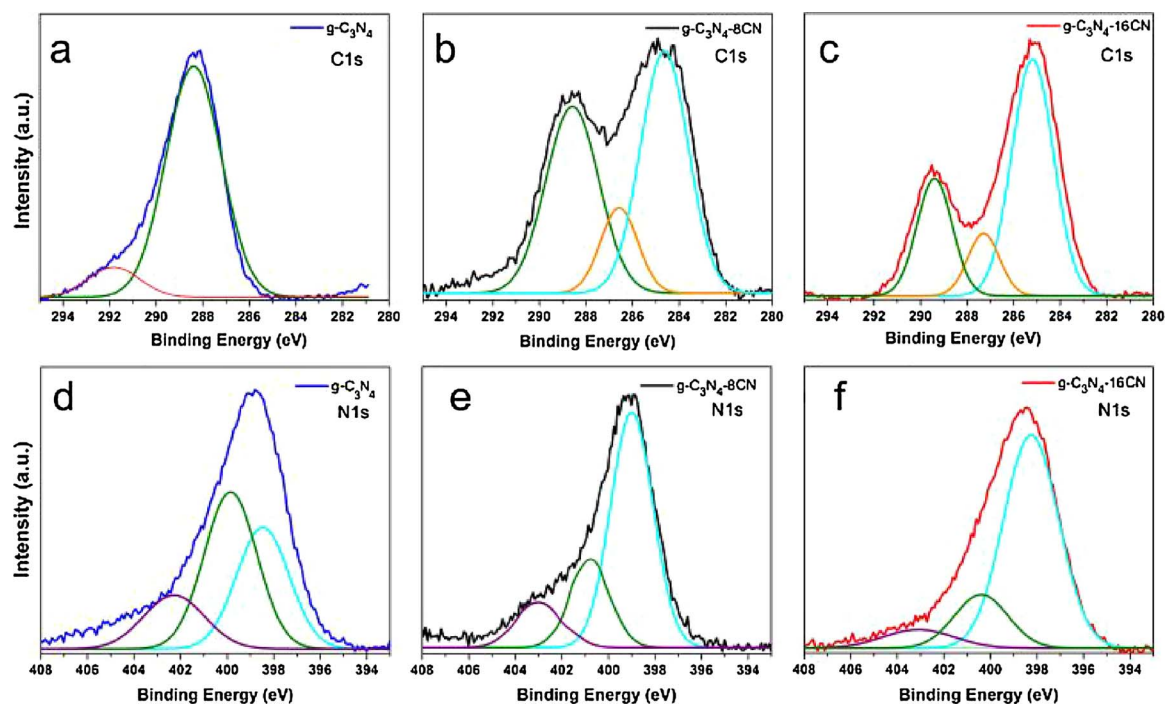


Fig. 2. C 1s (a–c), N 1s (d–f) X-ray photoelectron spectroscopy (XPS) curves of g-C$_3$N$_4$ (blue), g-C$_3$N$_4$-8CN (black), g-C$_3$N$_4$-16CN (red). (For interpretation of the references to colour in this figure legend, the reader is referred to the web version of this article).
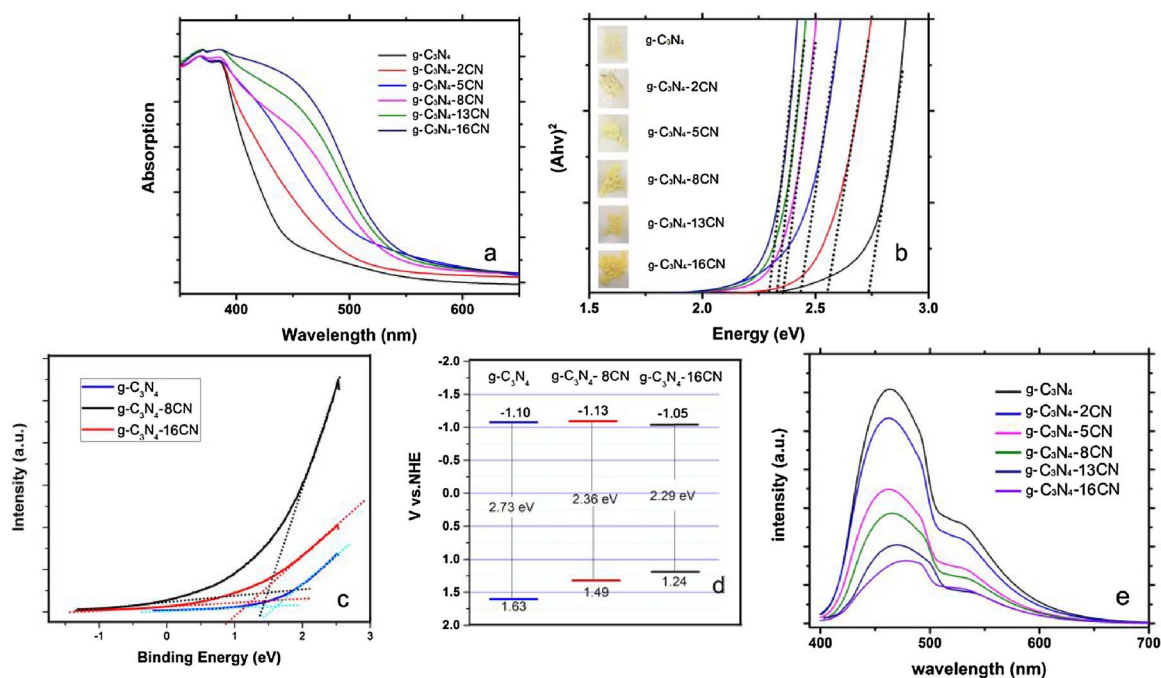
**Fig. 3.** (a) UV–vis absorption spectra of the g-C$_3$N$_4$-xCN samples; (b) Tauc's plot for g-C$_3$N$_4$-xCN samples; insets are the pictures of the samples showing gradual colour change; (c) Ultraviolet photoelectron spectra (UPS) of g-C$_3$N$_4$, g-C$_3$N$_4$-8CN and g-C$_3$N$_4$-16CN; (e) photoluminescence (PL) spectra of g-C$_3$N$_4$-xCN samples. (For interpretation of the references to colour in this figure legend, the reader is referred to the web version of this article).

were characterized by ultraviolet photoelectron spectroscopy (UPS). The valence-band maximum of g-C$_3$N$_4$, g-C$_3$N$_4$-8CN and g-C$_3$N$_4$-16CN is 1.53, 1.41, and 1.24 V (vs. NHE), respectively (Fig. 3c). With the above mentioned band gap values in hand, the conduction band minimum is thereby calculated to be −1.15, −0.95 and −1.05 V (vs. NHE). Cyanation of the carbon nitride thereby leads to a negative shift of the valence band maximum while keeping the conduction band minimum unchanged (Fig. 3d). To explore the radiative charge recombination and to learn about finer details of the band structure, photoluminescence (PL) spectra were measured as shown in Fig. 3e. For pristine g-C$_3$N$_4$, the strong PL emission at 470 nm shows fast charge carriers recombination. After cyanation, the intensity of this emission peak is weakened. This implies that the cyanation process reduces charge carriers recombination of the material. At the same time, the profile of the photoluminescence spectrum stays unchanged, which means that the higher positioned HOMO orbitals brought it by the nitriles are not really involved in radiative recombination. All this speaks for a rather stable localization of the photo-generated charges by means of the cyano groups.

Alkenyl sulfones are very important intermediates for in medicine chemistry [34,35]. The performance of the g-C$_3$N$_4$-xCN samples was therefore evaluated in the photocatalytic coupling reaction between styrene and sodium benzenesulfinate (Scheme 1) to afford alkenyl sulfones. There is no conversion without the photocatalysts. This photocatalytic coupling reaction shows a high selectivity of > 90%, in terms of the amount of styrene with the excess amount of sodium benzenesulfinate. Under UV light (365 nm) and blue light (445 nm) irradiation, both the pristine g-C$_3$N$_4$ and g-C$_3$N$_4$-16CN show high performance (Fig. 4), affording coupling product with yields around 90% (in terms of the amount of styrene), respectively. When using the green light (520 nm) as the energy source, the reaction with g-C$_3$N$_4$-16CN and
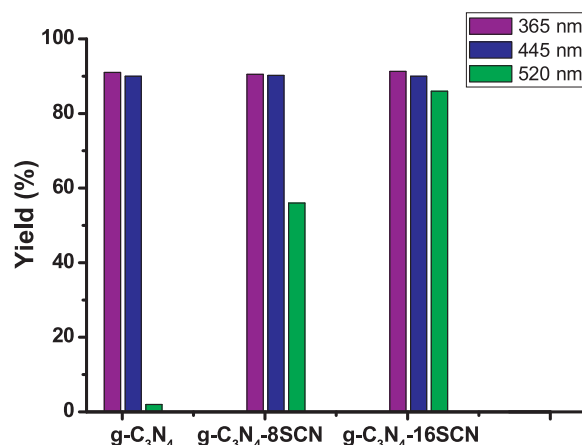


**Fig. 4.** Photocatalytic performance of the pristine g-C$_3$N$_4$ and g-C$_3$N$_4$-16SCN in the coupling reaction between styrene and sodium benzenesulfinate under UV (365 nm), blue (445 nm), green (520 nm), light and irradiation. Reaction conditions: 0.17 mmol of styrene 0.5 mmol of sodium benzenesulfinate and 0.34 mmol nitrobenzene were mixed with 5 mL ethanol in a glass vial. 25 mg of the photocatalyst were added in the reaction mixture as well. The glass reactor was then irradiated by different LED for 24 h. The yield of the reaction was determined by GC-MS/FID. (For interpretation of the references to colour in this figure legend, the reader is referred to the web version of this article).

g-C$_3$N$_4$-8CN still show satisfying yield of 88% and 56%, while the pristine g-C$_3$N$_4$ is almost inactive in such reaction condition, giving a negligible yield of 2%. Under the irradiation of orange light (590 nm), g-C$_3$N$_4$, g-C$_3$N$_4$-16CN and g-C$_3$N$_4$-8CN are inactive in this reaction, all presenting the yield of lower than 0.5%.
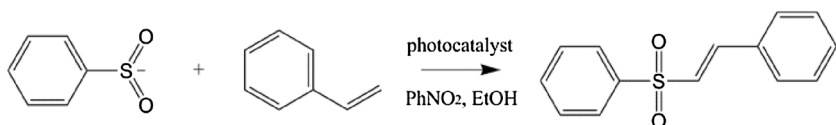


**Scheme 1.** Photocatalytic coupling reaction between styrene and sodium benzenesulfinate.

## 4. Conclusions

We presented a novel photocatalytic reaction to modify carbon nitride materials with cyano groups, using sodium thiocyanate in acetonitrile as the cyano group source. The cyano group content in the sample could be easily controlled by the concentration of the NaSCN. The cyanation modification takes place at former uncondensed amine groups and leads to a narrowed band gap as well as improved photo-induced charge carrier separation. The cyano group grafted carbon nitride shows a dramatically enhanced performance in mild photoredox reactions under green light, here exemplified by the photocatalytic coupling reaction between styrene and sodium benzenesulfinate, which is in stark contrast with the spectrally limited reactivity of pristine g-$C_3N_4$. This work not only offers a methodology for enhancing the visible light response of the carbon nitride materials, but also sheds light on the possibilities of designing novel carbon nitride materials by attaching favourable donor and acceptor groups on the carbon nitride scaffold via chemical/photochemical reactions pathways.

## Acknowledgement

## Appendix A. Supplementary data

Supplementary material related to this article can be found, in the online version, at doi:https://doi.org/10.1016/j.apcatb.2018.01.065.

## References

[1] W.-J. Ong, L.-L. Tan, Y.H. Ng, S.-T. Yong, S.-P. Chai, Chem. Rev. 116 (2016) 7159–7329.
[2] G. Dong, Y. Zhang, Q. Pan, J. Qiu, J. Photochem. Photobiol. C 20 (2014) 33–50.
[3] D. Dontsova, C. Fettkenhauer, V. Papaefthimiou, J. Schmidt, M. Antonietti, Chem. Mater. 28 (2016) 772–778.
[4] Z. Pei, J. Zhao, Y. Huang, Y. Huang, M. Zhu, Z. Wang, Z. Chen, C. Zhi, J. Mater. Chem. A 4 (2016) 12205–12211.
[5] X. Fu, X. Hu, Z. Yan, K. Lei, F. Li, F. Cheng, J. Chen, Chem. Commun. 52 (2016) 1725–1728.
[6] V.Wh. Lau, D. Klose, H. Kasap, F. Podjaski, M.C. Pignié, E. Reisner, G. Jeschke, B.V. Lotsch, Angew. Chem. Int. Ed. 56 (2017) 510–514.
[7] G. Gao, Y. Jiao, E.R. Waclawik, A. Du, J. Am. Chem. Soc. 138 (2016) 6292–6297.
[8] K. Li, B. Peng, J. Jin, L. Zan, T. Peng, Appl. Catal. B 203 (2017) 910–916.
[9] G. Zhang, A. Savateev, Y. Zhao, L. Li, M. Antonietti, J. Mater. Chem. A 5 (2017) 12723–12728.
[10] T.Y. Ma, J. Ran, S. Dai, M. Jaroniec, S.Z. Qiao, Angew. Chem. Int. Ed. 54 (2015) 4646–4650.
[11] J. Xu, T.J. Brenner, Z. Chen, D. Neher, M. Antonietti, M. Shalom, ACS Appl. Mater. Interfaces 6 (2014) 16481–16486.
[12] Z. Lin, X. Wang, Angew. Chem. Int. Ed. 52 (2013) 1735–1738.
[13] X.-H. Li, M. Antonietti, Chem. Soc. Rev. 42 (2013) 6593–6604.
[14] J. Hou, H. Cheng, C. Yang, O. Takeda, H. Zhu, Nano Energy 18 (2015) 143–153.
[15] Y. Zhang, T. Mori, J. Ye, M. Antonietti, J. Am. Chem. Soc. 132 (2010) 6294–6295.
[16] X. Yang, H. Tang, J. Xu, M. Antonietti, M. Shalom, ChemSusChem 8 (2015) 1350–1358.
[17] P. Zhang, H. Li, Y. Wang, Chem. Commun. 50 (2014) 6312–6315.
[18] M. Shalom, M. Guttentag, C. Fettkenhauer, S. Inal, D. Neher, A. Llobet, M. Antonietti, Chem. Mater. 26 (2014) 5812–5818.
[19] J. Wen, J. Xie, X. Chen, X. Li, Appl. Surf. Sci. 391 (2017) 72–123.
[20] B. Jin, G. Yao, X. Wang, K. Ding, F. Jin, ACS Sustain. Chem. Eng. 5 (2017) 7260–7268.
[21] Z. Mo, H. Xu, Z. Chen, X. She, Y. Song, J. Wu, P. Yan, L. Xu, Y. Lei, S. Yuan, H. Li, Appl. Catal. B 225 (2018) 154–161.
[22] H. Yu, R. Shi, Y. Zhao, T. Bian, Y. Zhao, C. Zhou, G.I. Waterhouse, L.Z. Wu, C.H. Tung, T. Zhang, Adv. Mater. 29 (2017).
[23] Z. Hong, B. Shen, Y. Chen, B. Lin, B. Gao, J. Mater. Chem. A 1 (2013) 11754–11761.
[24] V.W.-h. Lau, I. Moudrakovski, T. Botari, S. Weinberger, M.B. Mesch, V. Duppel, J. Senker, V. Blum, B.V. Lotsch, Nat. Commun. 7 (2016) 12165.
[25] P. Niu, L.C. Yin, Y.Q. Yang, G. Liu, H.M. Cheng, Adv. Mater. 26 (2014) 8046–8052.
[26] H.L. Lee, Z. Sofer, V. Mazánek, J. Luxa, C.K. Chua, M. Pumera, Appl. Mater. Today 8 (2016) 150–162.
[27] M. Rueping, S. Zhu, R.M. Koenigs, Chem. Commun. 47 (2011) 12709–12711.
[28] T. Castanheiro, J. Suffert, M. Donnard, M. Gulea, Chem. Soc. Rev. 45 (2016) 494–505.
[29] I. Wilson, G. Harris, J. Am. Chem. Soc. 83 (1961) 286–289.
[30] R. Jenny, M. Botz, D. Dimitriadis, T. Polglase, W. Phillips, Miner. Metall. Proc. 18 (2001) 126–132.
[31] A. Majumdar, S.C. Das, T. Shripathi, R. Hippler, Compos. Interfaces 19 (2012) 161–170.
[32] M. González-Torres, M.G. Olayo, G.J. Cruz, L.M. Gómez, V. Sánchez-Mendieta, F. González-Salgado, Adv. Chem. 71 (2014) 3057—3287.
[33] X. Miao, X. Yan, D. Qu, D. Li, F. Tao, Z. Sun, ACS Appl. Mater. Interfaces 9 (2017) 18549–18556.
[34] A.U. Meyer, V.W. Lau, B. König, B.V. Lotsch, Eur. J. Org. Chem. 15 (2017) 2179–2185.
[35] A.U. Meyer, S. Jäger, H.D. Prasad, Adv. Synth. Catal. 357 (2015) 2050–2054.